Design of Cell-Permeable Stapled Peptides as HIV-1 Integrase Inhibitors

Ya-Qiu Long,*,[†] Shao-Xu Huang,[†,‖] Zahrah Zawahir,[‡,‖] Zhong-Liang Xu,[†] Huiyuan Li,[†] Tino W. Sanchez,[‡] Ying Zhi,[†] Stephanie De Houwer,[§] Frauke Christ,[§] Zeger Debyser,[§] and Nouri Neamati*,[‡]

[†]CAS Key Laboratory of Receptor Research, Shanghai Institute of Materia Medica, Chinese Academy of Sciences, 555 Zuchongzhi Road, Shanghai 201203, China

[‡]Department of Pharmacology and Pharmaceutical Sciences, School of Pharmacy, University of Southern California, 1985 Zonal Avenue, Los Angeles, California 90033, United States

[§]The Laboratory for Molecular Virology and Gene Therapy, KU Leuven and IRC KULAK, Kapucijnenvoer 33, B-3000 Leuven, Flanders, Belgium

S Supporting Information
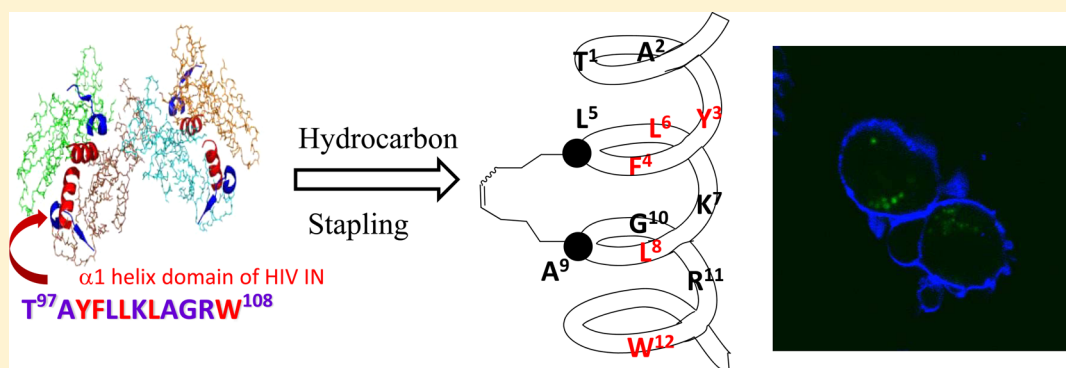
ABSTRACT: HIV-1 integrase (IN) catalyzes the integration of viral DNA into the host genome, involving several interactions with the viral and cellular proteins. We have previously identified peptide IN inhibitors derived from the α-helical regions along the dimeric interface of HIV-1 IN. Herein, we show that appropriate hydrocarbon stapling of these peptides to stabilize their helical structure remarkably improves the cell permeability, thus allowing inhibition of the HIV-1 replication in cell culture. Furthermore, the stabilized peptides inhibit the interaction of IN with the cellular cofactor LEDGF/p75. Cellular uptake of the stapled peptide was confirmed in four different cell lines using a fluorescein-labeled analogue. Given their enhanced potency and cell permeability, these stapled peptides can serve as not only lead IN inhibitors but also prototypical biochemical probes or "nanoneedles" for the elucidation of HIV-1 IN dimerization and host cofactor interactions within their native cellular environment.

■ INTRODUCTION

HIV-1 integrase (IN) efficiently inserts viral DNA into the host genome in two catalytic events. The first step, 3′-processing, involves the cleavage of a dinucleotide adjacent to a conserved CA on each terminus of the reverse-transcribed DNA, leaving the recessed 3′-hydroxyl groups. In the subsequent strand transfer step, these hydroxyl groups carry out a nucleophilic attack on the host DNA.[1−3] This results in a stable and irreversible integration of the proviral DNA in the host genome. Because IN has no mammalian counterpart, it is an attractive therapeutic target. Currently, raltegravir and elvitegravir are the two approved drugs selectively targeting IN and additional ones are being tested in clinical studies.[4−7] All catalytic events preceding integration (from viral fusion to formation and nuclear import of the large nucleoprotein complex termed the

preintegration complex (PIC)), as well as the integration itself, are mediated by protein−protein interactions between relevant viral proteins and host cell cofactors.[8] IN is known to participate in several of these functional interactions with cellular proteins such as gemin2, cyclin-dependent kinase inhibitor p21, transportin-SR2, and the extensively studied lens epithelium-derived growth factor (LEDGF/p75).[9−15] Selectively targeting these vital interactions as well as the IN dimerization/multimerization step as a therapeutic strategy against HIV-1 using peptidomimetic, biologically stable analogues of active peptides, or small-molecule inhibitors, is a rapidly developing field of interest that benefits significantly

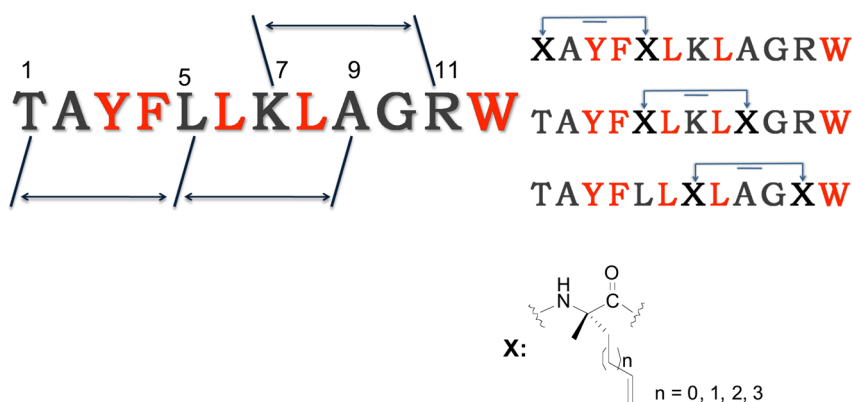**Figure 1.** Optional positions on **NL6** incorporating the α,α-disubstituted amino acids for side chain bridging. The red letters represent the essential residues for the IN dimerization.

from novel research into biochemical probes or "nano-needles".[12] Given the powerful ability of the ubiquitous α-helical motif in mediating intracellular protein–protein interactions across extensive biological pathways, such structurally immutable chemical tools may have general utility in further clarification and/or selective modulation of such protein–protein interactions within their native cellular environment. Unfortunately, most peptides are not suitable probes for in vivo studies because of their poor cellular uptake. However, when they are stapled into conformationally restricted analogues, they can penetrate cellular membrane like biological needles.

Previous studies from this group have demonstrated that peptides can interfere with the IN catalysis, as well as with the key LEDGF/p75–IN interaction necessary for successful integration.[16–18] A peptide derived from the reverse transcriptase region of the HIV-1 *HXB2 Pol* sequence showed low micromolar inhibition of IN activity.[16] Inhibition of the LEDGF/p75 interaction was demonstrated with both wild-type and mutant IN proteins in vitro by a peptide derived from the LEDGF/p75 protein sequence containing two IN contact "hotspots".[18] Finally, we used a "sequence-walking" strategy to pinpoint the areas of catalytic interest on wild-type IN protein. Evaluation of the inhibition of IN catalysis by a series of peptides spanning the IN protein sequence resulted in the identification of two peptides, **NL6** and **NL9**, with low micromolar IC_{50} values for the inhibition of HIV-1 IN catalysis.[17] Each peptide was derived from the $\alpha1$ and $\alpha3$ helical domains of the IN protein, respectively. Alanine scanning on these peptides further pinpointed the amino acid residues that were later proven to be critical for IN dimerization and at least one known HIV-1 IN protein–protein interaction, that of LEDGF/p75 and IN.[18,19] While these studies all provide excellent examples of the potential of peptides in drug development, the notorious issues of poor cell permeability, secondary structure instability, and in vivo proteolysis severely compromise peptides as successful therapeutic agents.

The two most potent inhibitory IN-derived α-helical peptides from the latter study are the focus of this report. By examining the two-domain crystal structures of IN,[20,21] we found that the central core dimers are linked via interactions of various types and the interfacial region of dimeric IN involves the strong helix-to-helix contacts $\alpha1:\alpha5'$ and $\alpha5:\alpha1'$.[22,23] Because our peptide **NL6** just falls within the sequence of the $\alpha1$ helical domain, we propose that α-helix stabilization on **NL6** via a hydrocarbon "staple" might enhance the interfacial

interaction and cell permeability. This all-hydrocarbon stapled α-helix peptide strategy was first reported by the Verdine group to enhance the helicity and metabolic stability of peptides,[24] then was successfully used to generate a series of helical, protease-resistant, cell permeable peptides derived from the amphipathic helical BH3 region found in members of the family of BCL-2 proteins.[25–27] A stapled BH3 domain peptide from the BID protein specifically activated the apoptotic pathway in leukemia cells and human leukemia xenograft models.[25] However, a more recent study concluded that hydrocarbon stapled BimBH3 peptide neither increased binding affinity nor enhanced cell permeability compared to the unstapled peptide.[27] This is in sharp contrast to the original studies by Walensky et al.[25] Recently, a stapled p53 peptide was shown to directly modulate the transcriptional activity in hDM2-over-expressing cancer cells by reactivation of the p53-mediated tumor suppressor pathway.[28,29] Both approaches apply to cancer disease models. A proof-of-concept cell-penetrating peptide targeting the HIV-1 capsid particle assembly was also described that crossed the cell membrane and bound to the C-terminal domain of the HIV-1 capsid protein.[30] Cell permeability enhancement strategies for peptides include the conjugation of positively charged protein-transduction domains such as the Tat-peptide conjugation, the antennapedia homeodomain of *Drosophila*, and poly arginine segments.[31,32] Cyclization techniques to enforce the α-helical nature of many peptides have also been demonstrated. Furthermore, side chain and backbone cyclization of peptides is another way to improve the stability of linear peptides and examples of such peptides were reported to inhibit the IN catalytic activities.[33–35] However, polar cross-links often limit cell permeability and leave the peptides open to degradation.[36,37] The hydrocarbon stapling technique elegantly combines enhanced cell penetration of structurally stable α-helical peptides with an increased resistance to proteolytic degradation. We thus synthesized a series of **NL6** derived peptides each containing hydrocarbon "staples" of different lengths in an attempt to induce and stabilize their helical conformation and consequently enhance their cell permeability.

This report identifies three α-helix stabilized IN-derived peptides inhibiting the HIV-1 replication in the infected cells. The corresponding unstapled peptides do not show therapeutically selective inhibition of the replication in cell-based assays, although each pair of peptides has similar activity against IN in our enzymatic assay. These peptides also inhibit the LEDGF/p75–IN interaction in vitro. More significantly, the fluores-

cently labeled stapled peptide is readily taken up by the cells. To our knowledge this is the first report attempting to design and synthesize all-hydrocarbon stapled peptides targeting the integration events either by directly inhibiting IN or by inhibiting its interaction with LEDGF/p75.

RESULTS

The side chain bridging is an effective approach to induce and stabilize the α-helix conformation of the linear peptide, and the all-hydrocarbon bridge enables metabolic stability and cell membrane permeability. Rather than stabilizing preferred conformations, under certain circumstances, an all-hydrocarbon staple can interact with the surface of the target protein and contribute to the binding interaction.[29] Incorporation of α,α-disubstituted olefinic amino acids at i and $i + 4$ positions of the 12-amino acid **NL6** sequence followed by a ruthenium-catalyzed ring-closing metathesis (RCM) reaction generated hydrocarbon stapled IN peptides.[38] The α-methyl-α-alkenyla-mino acid substitutions were made to flank three (substitution positions i and $i+4$) amino acids within the **NL6** peptide so that reactive olefinic residues would reside on the same face of the α-helix. Furthermore, the olefinic side chain varied from 3- to 6-methylene to determine an optimal chain length for the hydrocarbon staple.

We sought to optimize the **NL6** peptide as a biological tool and a prototype therapeutic by enforcing its α-helical structure while preserving the key interacting residues that enable the specific IN engagement. Therefore, the inserted position of the α,α-disubstituted unnatural amino acid was chosen to avoid the essential IN-binding residues based on our previous alanine scanning results.[17] As shown in Figure 1, three types of all-hydrocarbon chain-tethered cyclic peptides were synthesized, with N-terminal, middle, and C-terminal incorporation, respectively, to determine which position is favorable for the formation of the α-helix. Then the hydrocarbon cross-link length was investigated to achieve the best helix-stabilizing and potency-enhancing effects while the optimal inclusion positions of the two α,α-disubstituted amino acids into **NL6** peptide were held constant.

Efficient Synthesis of Chiral α,α-Disubstituted Amino Acids Bearing Olefinic Tethers of Various Lengths and a Panel of Hydrocarbon-Stapled Peptides with Different Inserted Position and Cross-Link Length. In order to produce a series of hydrocarbon-stapled peptides for an enhanced α-helicity and metabolic stability, we established an efficient and facile methodology to synthesize optically pure α-methyl-α-alkenylamino acids suitably protected for solid phase peptide synthesis by optimizing the Seebach's oxazolidinone methods[39–41] and screening the alkylation conditions. As depicted in Scheme 1, starting from D-alanine, the condensation of N^{α}-Cbz-D-alanine with benzaldehyde dimethyl acetal under acidic conditions yielded predominantly cis-oxazolidinone followed by the enantioretentive alkylation under basic conditions.[40] The resulting 2-phenyl-4-methyl-substituted oxazolidinone underwent sequential hydrolysis and N-Fmoc protection to afford the desired products (S)-**4a–d**. Since previously modified conditions of benzaldehyde dimethyl acetal and BF₃·Et₂O required 4 days under −40 °C to achieve good yield and high diastereoselectivity,[42] an optimized condition by employing ZnCl₂ as the Lewis acid in combination with thionyl chloride greatly accelerated the predominant production of the desired cis-(2R,4R)-2-phenyl-4-methyloxazolidinone **1** only after 4 h of stirring at 0 °C.[43]

Scheme 1. Optimized Synthetic Route toward α-Methylated α-Amino Acids Bearing an Olefinic Side Chain of Various Lengths Suitably Protected for Solid Phase Peptide Synthesis[a]
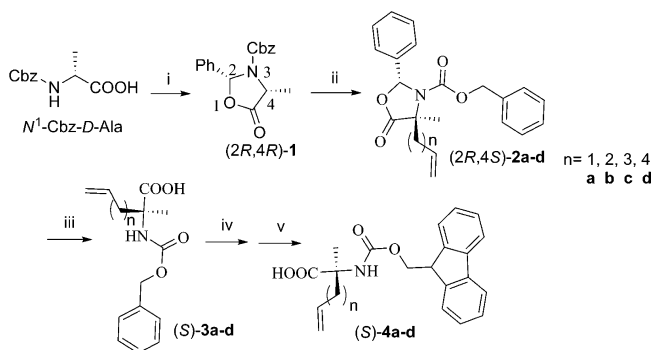
[a]Reagents and conditions: (i) PhCH(OMe)₂, SOCl₂, ZnCl₂, THF, 0 °C, 4 h, 77%; (ii) allyl bromide for **2a**, alkenyl iodide for **2b–d**, LiHMDS, THF/HMPA = 4:1, −78 °C, 4 h, 24−61%, dr 5:2; (iii) LiOH·H₂O, THF/H₂O = 3:1, 0−25 °C, 12 h, 85−100%; (iv) Ba(OH)₂·8H₂O (4.5 equiv for **3a−c**, 2.5 equiv for **3d**), H₂O/DME = 5:3, under N₂, refluxing, 12 h; (v) Fmoc-OSu, K₂CO₃, H₂O/acetone = 1:1, 25 °C, 2 h, 59−94% overall yield for two steps.

More effort was spent on the optimization of the alkylation reaction to the oxazolidinone core by the inert alkenyl halide that always gave poor yield when applying the reported conditions.[40,41] After the base, electrophile species, reagent ratio, reaction temperature, and solvent were screened, the best yield was obtained by using LiHMDS (2 equiv) as the base, alkenyl iodide as the electrophile, and anhydrous THF/HMPA (4:1, v/v) as the solvent at −78 °C. It is noteworthy that the addition sequence of the reagents greatly impacted the alkylation yield. Considering that the enolate intermediate was not stable and the alkylation was slow, we added the base separately to the prestirred mixture of the oxazolidinone and the alkenyl halide in THF/HMPA. Gratifyingly, this resulted in a stable and sufficient production of the alkylation products **2a−d** bearing alkenyl side chain of various length at the α-carbon, with a diastereomeric ratio of 5:2 regardless of the alkenyl chain length. This is consistent with the previously reported diastereoselectivity for a similar alkylation reaction.[43] Then the sequential hydrolysis by LiOH, the removal of the N^{α}-Cbz group with Ba(OH)₂ in DME/H₂O, and the N^{α}-Fmoc reprotection readily furnished the chiral α-methylated α-amino acids bearing an olefinic side chain with various chain lengths and with orthogonal protection suitable for solid-phase peptide synthesis based on Fmoc chemistry.

Subsequently, the α-methyl-α-alkenylamino acid containing linear peptide was assembled on the solid phase and the RCM reaction was performed on the resin with the assistance of microwave irradiation by using CEM Liberty peptide synthesizer (Scheme 2). However, for the introduction of the bulky α-methyl-α-alkenylamino acid, manual and double coupling was employed to secure the completion of the assembly. Generally, the metathesis reaction proceeded smoothly with the peptides containing the 4-carbon to 6-carbon long alkenyl tethers to generate corresponding 6-carbon to 10-carbon cross-linked peptides. However, the 3-carbon olefinic tether was too short to metathesize (**NLH10**). Both cis and trans double bond isomers were formed after the RCM

Scheme 2. Fmoc-Based Solid-Phase Synthesis of Unstapled, Stapled, and Fluorescently Labeled Peptides, Exemplified by the Synthesis of NLH5, NLH6, and NLX-1
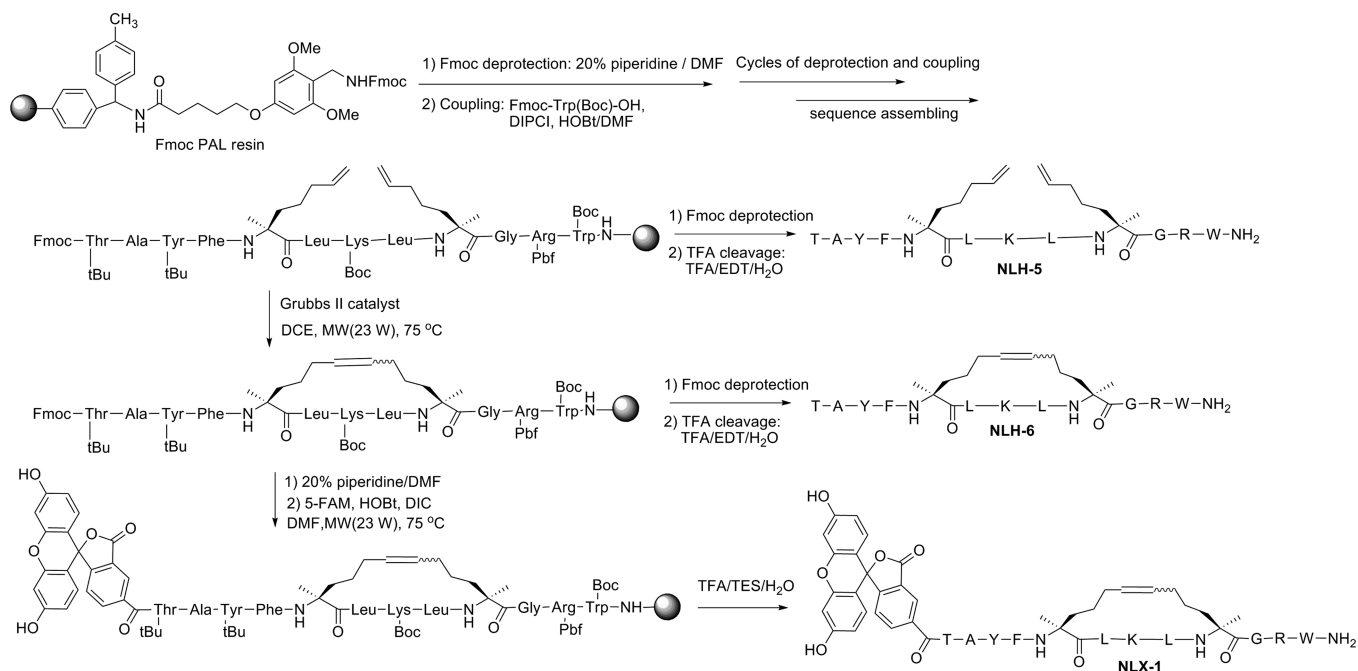
reaction, which were directly used in the following studies because they were not separable on HPLC.

The most potent stapled peptide **NLH6** was chosen to attach a fluorescein tag to monitor its subcellular distribution. Thus, the fluorescein-conjugated stapled peptide (**NLX-1**) was synthesized on the resin after the RCM reaction (Scheme 2). The coupling of 5-carboxyfluorescein with the side chain protected peptide on resin was achieved by using DIC and HOBt as the coupling agents with the microwave assistance. Then treatment of the resin-bound fluorescein-conjugated peptide with the cleavage cocktail afforded the fluorescently labeled stapled peptide **NLX-1**. Similarly, the linear peptide **NL6** was conjugated with fluorescein to yield **NLX-2** to serve as a negative control.

Appropriate Hydrocarbon Stapling Increases the α-Helical Propensity of the IN Peptides. The circular dichroism (CD) spectra of the linear and conformationally constrained peptides were measured in the solvent system of CH_3CN/PBS (40% v/v), and the select CD spectra are shown in Figure 2. The organic solvent acetonitrile was added to improve the solubility of the peptide in the PBS buffer at pH 7.2. The presence of acetonitrile might interfere with the formation of α-helix conformation of the peptide in the solution. Studies on peptide fragments have revealed that acetonitrile stabilizes and induces β-sheet conformation.[44] However, considering the solubility and the small amount of the acetonitrile employed, we believe that the CD spectra can still reflect the real trend of the conformational change of the stapled peptides. The α-helical content measured by CD is based on a method reported previously (Table 1).[45]

As expected, for these 12-amino acid **NLH** series with i, i + 4 spanning pattern, the hydrocarbon stapled peptides generally demonstrated an improved α-helical content (23−49% α-helicity) compared to the parent **NL6** linear peptide that displayed 20% α-helical content in 40% CH_3CN/H_2O solution and thus predominantly existed as a random coil (Figure 2 and Table 1). The exception is the short hydrocarbon stapled
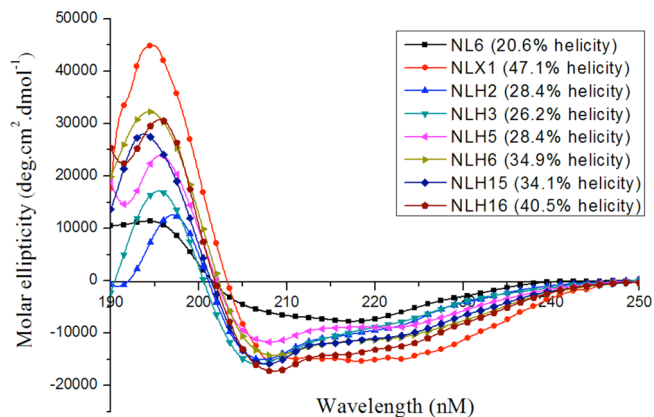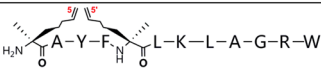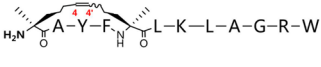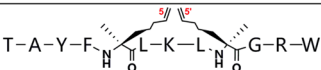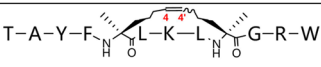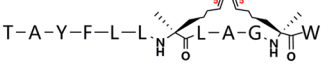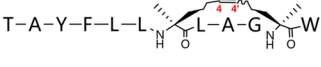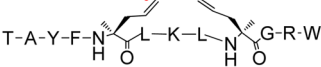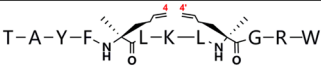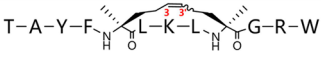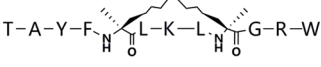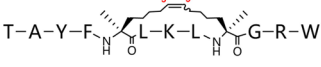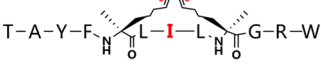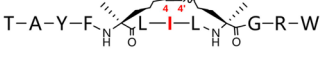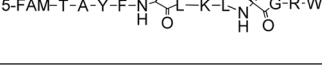

Figure 2. CD spectra of the select peptides with incorporation of two α,α-disubstituted amino acids (i, i + 4) in unstapled and stapled forms.

peptides (**NLH11** and **NLH12**) that might be too rigid to achieve the desired conformation of the whole molecule. Interestingly, the fluorescein-tagged stapled peptide (**NLX-1**) displayed the highest α-helical content, probably because of the N-capping effect of the bulky hydrophobic fluorescent group. On the other hand, the inserted position of the α,α-disubstituted amino acid strongly affected the formation of α-helix conformation, with the middle position being optimal for the stabilization of α-helix geometry. For example, a consistent increase in the α-helical content was observed on the middle cross-linked peptides relative to the corresponding unstapled modified peptides (**NLH6** vs **NLH5**, **NLH14** vs **NLH13**, **NLH16** vs **NLH15**). The chain length of the hydrocarbon cross-link also affected the induction of α-helix conformation. Among the 4-, 5-, and 6-methylene olefinic side chains, the pentene side chain turned out to be the best length with respect to inducing and stabilizing the α-helix conformation of the HIV-1 IN 12-mer peptide **NL6** (**NLH6** vs **NLH12**, **NLH14**). The hydrocarbon staple of 6 carbons is too short to permit the

Table 1. Structures and the α-Helical Content of the Peptides with α,α-Disubstituted Amino Acid Incorporation[a]

Peptide	Sequence	α-Helix
NL6	T–A–Y–F–L–L–K–L–A–G–R–W	20.6
NLH2		28.4
NLH3		26.2
NLH5		28.4
NLH6		34.9
NLH8		40
NLH9		38
NLH10		18
NLH11		14
NLH12		8
NLH13		26.2
NLH14		30.6
NLH15		34.1
NLH16		40.5
NLX1		47.1

[a]The CD spectra of NL-6 and NLH series were recorded in 10 mM PBS (pH 7.2)/40% MeCN (v/v) at room temperature. Peptides were dissolved at 200 μM. PBS: phosphate buffered solution, 10 mM, pH 7.2.

formation of an unstrained helix and that of 10 carbons is longer than necessary and therefore does not constrain the helix as effectively as the 8-carbon tether. In short, for the *i, i + 4* stapled peptide series, the incorporation of the α,α-disubstituted amino acids at the middle positions of the sequence and the cross-link of 8 carbons provide the optimal fits for stapling the HIV-1 IN peptide to achieve enhanced helicity.

α-Helical Peptide Pairs Inhibit IN Catalytic Activities. The sequences of each stapled α-helix stabilized peptide and its corresponding unstapled peptide are shown in Table 1, and their activities are shown in Table 2. Each pair contains a covalent hydrocarbon staple spanning the *i, i + 4* positions whose residues were not essential for the HIV-1 inhibitory activity according to the alanine scanning results.[17] The position of residue *i* in each peptide pair varies, with *i* in the first pair being the threonine residue at the N-terminus of the

Table 2. Inhibition of HIV-1 IN Catalytic Activity, Its Interaction with LEDGF/p75, and Viral Replication by Conformationally Constrained α-Helical Peptides and Their Corresponding Unrestrained Analogues

peptide	3′-processing IC$_{50}$ (μM)^a	strand transfer IC$_{50}$ (μM)	EC$_{50}$ (μM)^b	CC$_{50}$ (μM)^c	therapeutic index^d	LEDGF/p75−IN IC$_{50}$ (μM)^e
NLH2	22 ± 8	15 ± 5	5	5	NA^f	26
NLH3	53 ± 15	19 ± 10	4	25	6	>100
NLH5	9 ± 1	6 ± 1	28	28	NA^f	15
NLH6	9 ± 1	6 ± 1	20	50	3	14
NLH8	>100	>100	NT^g	NT^g	NA^f	NT^g
NLH9	>100	>100	NT^g	NT^g	NA^f	NT^g
NLH10	>333	>111	NT^g	NT^g	NA^f	NT^g
NLH11	74 ± 11	68 ± 5	>18	18	NA^f	20
NLH12	90	83	>40	40	NA^f	14
NLH13	61 ± 12	43 ± 5	NT^g	NT^g	NA^f	NT^g
NLH14	48 ± 10	44 ± 4	NT^g	NT^g	NA^f	NT^g
NLH15	15 ± 2	11 ± 3	11	18	1.6	>100
NLH16	22 ± 3	25 ± 7	5 ± 2	41 ± 15	8	5
NLX-1	5 ± 1	6 ± 1	11	>125	>11	25
NLX-2	17.5 ± 1.5	6.2 ± 0.2	13	70	5	25
NL6^h	21 ± 7	4 ± 1	18.7	>100	>5	>25

^{a}IC$_{50}$: 50% inhibition of the integrase enzymatic activity. ^{b}EC$_{50}$: 50% cytoprotective activity of the peptides in HIV-1 infected cells. ^{c}CC$_{50}$: 50% cell death in same cells. ^{d}Therapeutic index: ratio of CC$_{50}$ to EC$_{50}$ values. ^{e}LEDGF/p75 IC$_{50}$: 50% inhibition of the interaction between the two proteins. ^{f}NA: not applicable. ^{g}NT: not tested. ^{h}Catalytic activities are cited from ref 17.

sequence TAYF**L**LKL**A**GR**W** (the residues in bold represent the irreplaceable hot spots). In the second peptide pair the position of residue *i* moves to the middle leucine residue, and the third peptide pair bears a C-terminal hydrocarbon staple with *i* being lysine. This change in position of the hydrocarbon linker has an effect on the inhibitory activity of the peptides, which is highly correlated with the α-helical conformation and the orientation of the essential residue side chain.

The most active peptide pair is **NLH5** (unstapled) and **NLH6** (stapled) with IC$_{50}$ values of 9 ± 1 μM for 3′-processing and 6 ± 1 μM for strand transfer. The staple on this pair is positioned linking the leucine residue (*i*) in the TAYF**L**L-KL**A**GR**W** sequence with the alanine residue (*i* + 4), resulting in a significant induction of α-helicity on the two peptides **NLH5** and **NLH6**. In contrast, the least active peptide pairs are **NLH8** (unstapled) and **NLH9** (stapled), with IC$_{50}$ > 100 μM for both catalytic activities. They contain a hydrocarbon staple linking the lysine (*i*) with the arginine residue (*i* + 4) and possess the highest α-helical content. To understand the observation that the C-terminal stapling induced high propensity of α-helix conformation but caused a significant loss of the inhibitory potency, we calculated the possible conformations of the three peptides (**NLH9**, **NLH6**, and **NL6**) by running MM2/minimize energy through Chemoffice ChemBio3D Ultra 11.0. According to the calculated optimal conformation with minimized energy of the three peptides (not shown), the side chain of the essential residue Trp on peptide **NLH9** was distorted from that of the parent peptide **NL6** and of the active peptide **NLH6**, which might be the reason for the loss in activity. This observation is consistent with a recent report demonstrating that the addition of a hydrocarbon staple to the BimBH3 peptide did not enhance its binding affinity or biological activity presumably because of the loss of a network of stabilizing intramolecular interactions on the peptide.[27] Therefore, the orientation of the essential residue side chain is another important issue besides the active conformation stabilization for the protein−protein interactions.

The single substitution (K7I) on the **NL6** sequence was previously found to enhance the HIV-1 inhibitory activity.[17]

Stapling the **NL6** (K7I) at the middle produced the active peptide pair **NLH15** and **NLH16** with an increase in α-helicity, thus generating moderate activity against the 3′-processing and strand transfer reactions. Overall, the trends observed for the IN inhibitory activity for these stapled and unstapled peptides correlated reasonably well with their α-helical propensities (Table 2). Since HIV IN exerts its function as a multimer (IN dimers are sufficient for 3′-P, and tetrameric structures participate in the ST step),[46,47] presumably our active peptides inhibit both 3′-P and ST reactions by blocking the multimerization of the HIV IN.

Some Peptide Pairs Inhibit LEDGF/p75−IN Interaction. Interestingly, most of the peptide pairs active in inhibiting IN catalytic activities inhibited the LEDGF/p75−IN interaction as well, as shown in Table 2. Similar to the inhibition of IN catalysis, these peptide pairs showed comparable IC$_{50}$ values in the low micromolar range. The stapled peptide **NLH16** had an IC$_{50}$ of 5 μM. Its corresponding unstapled peptide **NLH15** does not show significant inhibition below 100 μM. Unstapled peptide **NLH2** inhibits the LEDGF/p75−IN interaction with an IC$_{50}$ of 26 μM, while its corresponding stapled partner **NLH3** is inactive. The peptide pair **NLH5** and **NLH6** and peptide pair **NLH11** and **NLH12**, with inclusion of the two α,α-disubstituted amino acids in the middle of the sequence, are all moderately active (IC$_{50}$ < 20 μM). Since the α1 helical domain of HIV IN is also involved in the interaction with LEDGF/p75 IBD (integrase binding domain),[48] not surprisingly, the α1 region-derived NL6 peptides inhibit the LEDGF/p75−IN interaction probably by binding to the LEDGF/p75 in a competitive fashion.

Stapled α-Helical Peptides Inhibit HIV-1 Replication. Six peptide pairs were each tested for the inhibition of HIV-1 replication in MT-4 cells. Cytotoxicity was also evaluated, and a therapeutic index was calculated for each peptide as a ratio CC$_{50}$/EC$_{50}$. Table 2 shows the EC$_{50}$, CC$_{50}$, and therapeutic indices for each of the peptides evaluated in this assay. From this group of pairs, the peptide showing the best overall therapeutic index of 8 is **NLH16** (stapled). **NLH16** thus inhibits the HIV-1 replication with the lowest corresponding
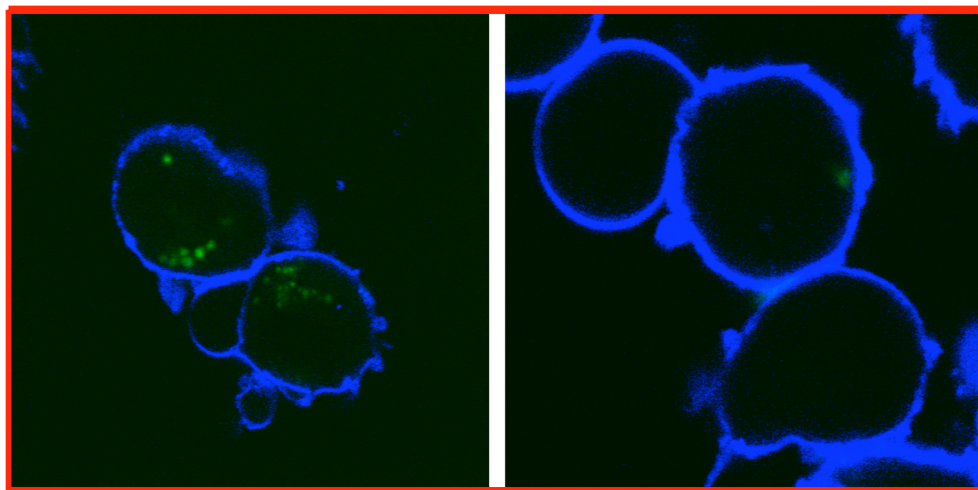
Figure 3. Uptake of the fluorescein-labeled peptides **NLX1** (A, left) and **NLX2** (B, right) in MT-4 cells. Images were generated using a Zeiss LSM510 microscope with a Plan-Apochromat 63×/1.4 oil DIC objective. The three-dimensional stacks were performed with Z step size of 0.3 mm using an argon laser for the measurement of FITC at 488 nm and a HeNe laser for the measurement of the cell membrane dye at 543 nm.
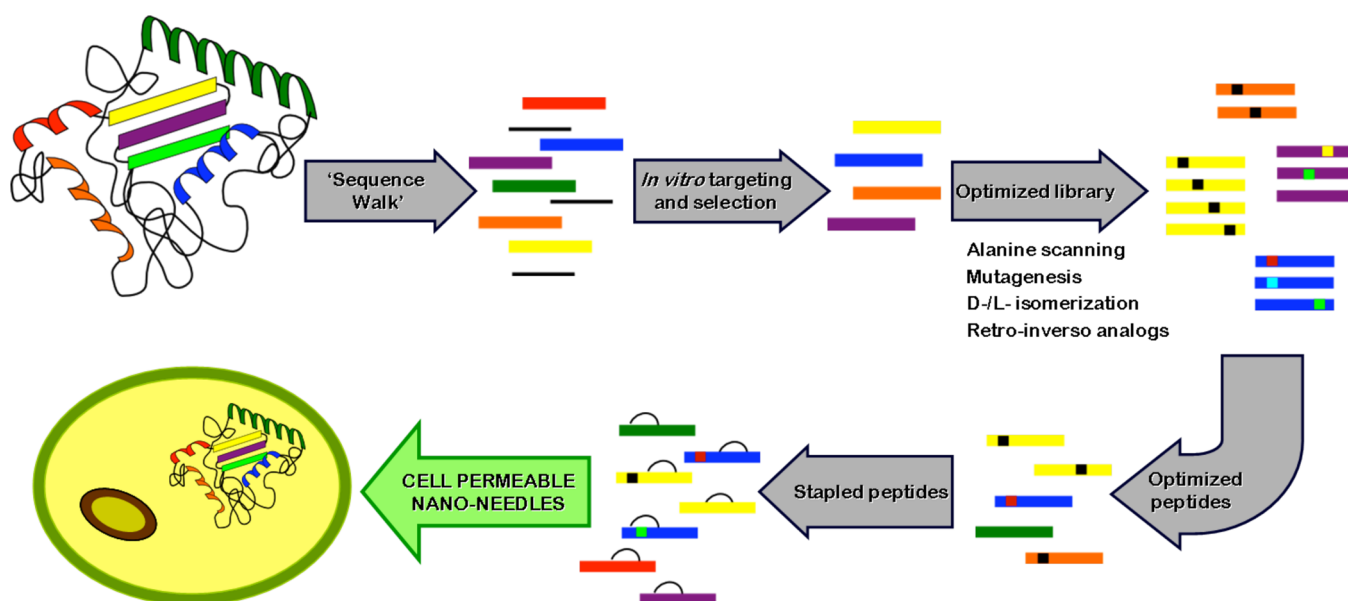

Figure 4. Strategy for design of cell permeable nanoneedles as probes toward elucidating regions of interest within a protein that are essential for efficient catalysis or protein−protein interactions.

cytotoxicity in MT4 cells. It contains an optimal 8-carbon hydrocarbon staple linking the leucine residue (i) in the middle of the sequence with an alanine residue (i + 4). Its corresponding unstapled peptide **NLH15** does not show therapeutically selective inhibition against the viral replication. Similar antiviral activity difference between the "open" and "closed" counterparts was observed on the peptide pairs **NLH2** and **NLH3**, **NLH5** and **NLH6**, in which the "closed" or stapled peptides inhibit the HIV-1 replication with less cytotoxicity than their corresponding open conformation derivatives. Interestingly, **NLH12** has the same sequence and contains the hydrocarbon staple spanning the same positions as peptides **NLH11** ("open" linker), **NLH5** (unstapled), and **NLH6** (stapled, closed). However, the shorter cross-link itself appears to cause a substantial loss in the inhibition of both IN catalysis and HIV-1 replication, which was consistent with the aforementioned observation that the 6-carbon staple of **NLH12** failed to stabilize the α helix conformation.

Peptides and peptide-like structures have the tendency to bind to cell surfaces and in some cases block the entry step of viral replication instead of acting on intracellular targets. We therefore determined the antiviral activity of **NLH16** against a viral strain that is resistant to entry inhibitors.[49] **NLH16** remains active against the AMD3100[50] resistant strain (EC_{50} = 4.3 μM). This suggests that the peptide may indeed enter the cell and show antiviral activity on an intracellular target. Because the stapled peptides significantly inhibit purified LEDGF/p75−IN, the antiviral effect is most likely due to the dual inhibition of IN and its interaction with LEDGF/p75. Peptides **NL6** and **NLX-2** do not cross the cell membrane (see below), and their antiviral activities are most likely due to the inhibition of viral entry. Future in-depth mechanistic studies will further elucidate their mechanism of action.

Stapled Peptides Are Cell Permeable. Stapled peptides are known to efficiently cross the plasma membrane. Because IN is an intracellular target, it is important to demonstrate

cellular uptake with any peptide targeting the integration events. Therefore, we conjugated a fluorescein tag on the N-terminus of the stapled peptide **NLH6** to generate **NLX-1** with a 72% yield. We further demonstrated that this fluorescent probe exhibits an enhanced α-helical content and significant IN inhibitory activity. In fact, **NLX-1** showed the highest (47%) α-helical content among all the synthesized peptides. To demonstrate the cellular uptake, we incubated two fluorescently labeled peptides **NLX-1** and **NLX-2** with MT-4 cells for 1 h. We observed a rapid accumulation of the stapled **NLX-1** peptide but not the unstapled **NLX-2** peptide in MT-4 cells (Figure 3A versus Figure 3B). To further illustrate a general trend for cellular uptake of the stapled peptide, we treated three additional cell lines (CEM, HCT116, and Panc-1 cells) with **NLX-1** for 3 h. Confocal microscopy and nuclear staining with Draq5 showed distinct cellular uptake of the stapled peptide (Figure S1 in Supporting Information). The uptake of **NLX-1** in all the cell lines was efficient and the peptide localized to the cytoplasm with minimum distribution to the nucleus.

DISCUSSION

Our strategy in the synthesis of these stapled peptides was to extrapolate to a cellular environment the idea established in our previous study that peptides derived from the protein of interest may be used to identify domains on the protein that are essential for catalytic activity, protein−protein interactions, and/or dimerization. Figure 4 summarizes this venture, from the synthesis of the original peptides, through the optimization for an enhanced activity, and the subsequent choice of peptides for the helix stabilization. While this idea has proven to be successful in our laboratory in vitro, we sought to extend it to cell-based assays by synthesizing hydrocarbon-stapled α-helical peptides. Such α-helix stabilized peptides mimicking the α-helical BH3 domain of the BCL-2 protein have previously been shown by Walensky et al. to have enhanced helicity compared to their unstapled counterparts.[25] These stapled peptides exhibit in vivo stability, as evidenced by their ability to suppress growth of human leukemia cells in mice by activating apoptotic pathways. For recent reviews and select applications of stapled peptides, see refs 51−55.

High throughput screening followed by structural optimization was essential in identifying IN inhibitors suitable for clinical use.[56] The complex protein−protein interactions of IN with cellular cofactors provide innovative therapeutic targets for the development of small-molecule inhibitors of HIV-1, which are regaded as an excellent alternative to the conventional active site-directed HIV-1 inhibitiors in the context of the rapid emergence of the viral cross-resistance. However, these targets are plagued by difficulties associated with the shallow, hydrophobic nature of the protein surfaces involved in such interactions.[54,55] A previous study by Brass et al. using RNAi and forward genetics techniques identified a plethora of HIV-dependency factors that are required for the HIV-1 infection.[57] We here introduce the concept of stapled optimized peptides as cell-permeable nanoneedles that will enable the identification of regions of interest in proteins that have thus far been identified as interacting protein partners of IN, and other viral proteins. The nanoneedles may themselves serve as a starting point for the development of novel inhibitors and may be further optimized for the inhibition of HIV-1 infection after formulation into nanoparticles and immunoliposomes. More importantly, nanoneedle technologies can be efficiently used to test the hypothesis of whether a given protein−protein

interaction is druggable. siRNA, shRNA, and antisense technologies are not effective in validating the importance of protein−protein interactions in a given disease, hampering efforts to find new targets. On the other hand, designing small-molecule inhibitors for protein−protein interaction is a challenging endeavor with the technologies currently available. This innovative concept of utilizing nanoneedles to both validate protein−protein interaction targets and discover novel therapeutics will prove to be highly efficient and cost-effective and will lead to the identification of new targets leading to new cures.

CONCLUSIONS

This study reports the first example of the all-hydrocarbon stapled peptides derived from the α-helical region of HIV-1 IN along the dimeric interface. We synthesized a series of stapled peptides and their corresponding unconstrained partners to compare and contrast their abilities to inhibit IN in enzymatic and cell-based assays. The stapled peptides show antiviral activity, while their corresponding unstapled peptides do not show therapeutically selective inhibition of viral replication in cell-based assays, although each pair of peptides has similar activity against purified IN. These peptides also inhibit the LEDGF/p75−IN interaction in vitro because of the fact that the IN region from which the peptide was derived corresponds to the site of the LEDGF/p75 binding. The active stapled peptide inhibits a viral strain resistant to an entry inhibitor, suggesting that its antiviral activity is due to intracellular targeting. More significantly, the fluorescently labeled stapled peptide was readily internalized by cells while the unstapled peptide was not taken up, demonstrating that the stapling enhances the cellular uptake. The antiviral activity of some linear peptides is most likely due to the nonspecific interference with viral entry but not due to the specific interaction with IN inside the infected cell. To our knowledge this is the first report on the design and synthesis of cell-permeable stapled peptides targeting the integration events by directly inhibiting IN or its interaction with the LEDGF/p75.

EXPERIMENTAL SECTION

Chemistry. ^{1}H NMR spectra were recorded on a Varian Mercury 300 or 400 MHz spectrometer. The data are reported in parts per million relative to TMS and referenced to the solvent in which they were run. EI mass spectra were obtained on a Finnigan MAT 95 mass spectrometer, and ESI mass spectra were recorded on a Finnigan LCQ Deca mass spectrometer. The solvent was removed by rotary evaporation under reduced pressure, and flash column chromatography was performed on silica gel H (10−40 μm). Anhydrous solvents were obtained by redistillation over sodium wire. The purity of all peptide products was >95% determined by analytical HPLC on a Waters 1525EF with Vydac 218TP C18 reversed-phase column (4.6 mm × 250 mm) in two solvent systems (system 1, solvent A, 0.05% TFA in water; solvent B, 0.05% TFA in 95% acetonitrile; system 2, solvent A, 0.05% TFA in water; solvent B, 0.05% TFA in methanol).

(2R,4R)-2-Phenyl-3-(carbobenzyloxy)-4-methyloxazolidin-5-one (1).[42] To a solution of Cbz-D-alanine (5 g, 22.4 mmol) and benzaldehyde dimethyl acetal (3.4 mL, 23 mmol) in dry THF (35 mL) at 0 °C was added thionyl chloride (1.79 mL, 24.6 mmol). After the mixture was stirred for 10 min, anhydrous ZnCl$_2$ (3.36 g, 24.6 mmol) was added, and the reaction mixture was stirred at this temperature for 4 h. The reaction mixture was quenched by dropwise addition of ice−water and adjusted to pH 5 with saturated NaHCO$_3$, then extracted with ether. The ether layer was washed with a saturated solution of NaHCO$_3$ and brine, dried over Na$_2$SO$_4$, and concentrated. The crude product was purified by crystallization from ethyl ether/n-hexane to

give the title compound **1** as colorless needles (5.38 g, 77%). Mp 52–53 °C. ^{1}H NMR (CDCl$_3$) δ: 1.59 (s, 3H), 4.47–4.52 (m, 1H), 5.14–5.21 (m, 2H), 6.65 (bs, 1H), 7.34–7.41 (m, 10 H). MS-EI: 311 (M$^+$).

(2R,4S)-2-Phenyl-3-(carbobenzyloxy)-4-methyl-4-(4-pentenyl)oxazolidin-5-one (2c). To a stirring solution of (2R,4R)-2-phenyl-3-(carbobenzyloxy)-4-methyloxazolidin-5-one **1** (2.446 g, 7.86 mmol) and 5-iodopent-1-en (2.004 g, 10.22 mmol) in dry THF/HMPA = 4: 1 (20 mL) was added LiHMDS (1 M, 15.7 mL, 15.7 mmol) in dry THF slowly and portionwise under nitrogen at −78 °C. This light yellow solution was stirred at this temperature for 2 h. Saturated NH$_4$Cl aqueous solution was added to quench the reaction. The THF was removed in vacuo. Then Et$_2$O was added to extract the solution. The organic layer was washed three times with saturated NaHCO$_3$ and NaCl solutions, respectively. The organic phase was dried over Na$_2$SO$_4$ and evaporated. The residue was purified by flash column chromatography with eluent of petroleum−ethyl acetate (5:1) to give compound **2c** (1.499 g, 50%) as a colorless oil. Further purification by recrystallization with Et$_2$O/hexane (3: 4) gave a colorless lumpy solid. Mp 59–60 °C; $[\alpha]^{20}_D$ +64.4° (c 0.38, CHCl$_3$). ^{1}H NMR (400 MHz, DMSO-d_6, 80 °C) δ: 1.16–1.31 (m, 2H), 1.67–1.79 (m, 4H), 1.91–2.00 (m, 2H), 2.24–2.33 (m, 1H), 4.93–5.09 (m, 4H), 5.65–5.75 (m, 1H), 6.59 (s, 1H), 7.05–7.46 (m, 10H). ^{1}H NMR (300 MHz, CDCl$_3$) two rotamers (5:2) δ: 1.16–1.39 (m, 4H), 1.72 (s, 0.85H), 1.82 (s, 2.14H), 2.05–2.24 (m, 1H), 2.48–2.70 (m, 1H), 4.90–5.09 (m, 3H), 5.54–5.84 (m, 1H), 6.44 (d, J = 24.7 Hz, 1H), 6.91 (d, J = 6.9 Hz, 1H), 7.15–7.50 (m, 10H). ^{13}C NMR (100 MHz, CDCl$_3$) δ: 23.91, 33.27, 35.49, 37.23, 67.48, 67.97, 89.54, 115.54, 126.96, 128.06, 128.36, 128.57, 128.93, 130.10. EI-MS m/z: 379 (M$^+$). HRMS-ESI m/z: calcd for C$_{23}$H$_{25}$NO$_4$ + Na 402.1681, found 402.1677.

Compounds **2a**, **2b**, and **2d** were prepared according to procedures similar to that for **2c**.

(2R,4S)-Benzyl 4-Allyl-4-methyl-5-oxo-2-phenyloxazolidine-3-carboxylate (2a). Starting from (2R,4R)-2-phenyl-3-(carbobenzyloxy)-4-methyloxazolidin-5-one (**1**) (3.113 g, 10 mmol), allyl bromide (2.420 g, 20 mmol) in 25.0 mL of THF/HMPA (4/1, v/v), and LiHMDS (1 M, 16.0 mL, 16 mmol), **2a** (2.148 g) was obtained as colorless oil in 61% yield. $[\alpha]^{20}_D$ +64.9° (c 1.14, CHCl$_3$). ^{1}H NMR (400 MHz, DMSO-d_6, 80 °C) δ: 1.72 (s, 3H), 2.48–2.50 (m, 1H), 3.06–3.09 (m, 1H), 5.01–5.20 (m, 4H), 5.61–5.72 (m, 1H), 6.46 (s, 1H), 7.12 (brs, 1H), 7.22 (s, 3H), 7.42–7.49 (m, 6H). ^{1}H NMR (300 MHz, CDCl$_3$) two rotamers (2.6:1) δ 1.71 (s, 0.82H), 1.80 (s, 2.15H), 2.53 (dd, J = 13.7, 6.2 Hz, 1H), 2.86–3.29 (m, 1H), 4.95 (s, 1H), 5.08–5.22 (m, 2H), 5.53–5.74 (m, 1H), 6.30 (d, J = 18.7 Hz, 1H), 6.87 (d, J = 6.2 Hz, 1H), 7.13–7.64 (m, 10H).

(2R,4S)-2-Phenyl-3-(carbobenzyloxy)-4-methyl-4-(but-3-enyl)oxazolidin-5-one (2b). Starting from **1** (1.557 g, 5 mmol), 4-iodobut-1-ene (1.365 g, 7.5 mmol) in 12.5 mL of THF/HMPA (4/1), and LiHMDS (1 M, 7.5 mL, 7.5 mmol), **2b** (0.431 g) was obtained as yellow oil in 24% yield. $[\alpha]^{20}_D$ +71.5° (c 1.03, CHCl$_3$). ^{1}H NMR (400 MHz, DMSO-d_6, 80 °C) δ: 1.67 (s, 3H), 1.81–1.96 (m, 3H), 2.36–2.39 (m, 1H), 4.93–5.07 (m, 4H), 5.62–5.72 (m, 1H), 6.56 (s, 1H), 7.10 (brs, 1H), 7.26 (s, 3H), 7.40–7.43 (m, 6H). EI-MS m/z: 365 (M$^+$).

(2R,4S)-2-Phenyl-3-(carbobenzyloxy)-4-methyl-4-(hex-5-enyl)oxazolidin-5-one (2d). Starting from **1** (2.179 g, 7 mmol), 6-iodohex-1-ene (1.900 g, 9.1 mmol) in 17.5 mL of THF/HMPA (4/1), and LiHMDS (0.5 M, 22.4 mL, 11.2 mmol), **2d** (1.122 g) was obtained as yellow oil in 41% yield. $[\alpha]^{20}_D$ +66.0° (c 0.97, CHCl$_3$). ^{1}H NMR (400 MHz, DMSO-d_6, 80 °C) δ: 1.09–1.33 (m, 4H), 1.67 (s, 3H), 1.70–1.78 (m, 1H), 1.95 (q, 2H), 2.27 (br, 1H), 4.92–5.09 (m, 4H), 5.70–5.80 (m, 1H), 6.56 (s, 1H), 7.12 (brs, 1H), 7.28 (s, 3H), 7.42 (s, 6H). ^{1}H NMR (300 MHz, CDCl$_3$) two rotamers (2.5:1) δ: 0.98–1.38 (m, 4H), 1.68 (s, 0.85H), 1.77 (s, 2.14H), 1.78–1.95 (m, 2H), 2.01–2.12 (m, 1H), 2.38–2.65 (m, 1H), 4.97 (m, 3H), 5.53–5.77 (m, 1H), 6.40 (d, J = 18.0 Hz, 1H), 6.87 (d, J = 6.3 Hz, 1H), 7.13–7.50 (m, 10H). EI-MS m/z: 393 (M$^+$).

2-(Benzyloxycarbonylamino)-2-methylhept-6-enoic Acid (3c). To a stirred solution of (2R,4S)- 2-phenyl-3-(carbobenzyloxy)-4-methyl-4-(4-pentenyl)oxazolidin-5-one **2c** (374 mg, 0.99 mmol) in

THF/H$_2$O (3:1, 20 mL) was added LiOH·H$_2$O (83 mg, 1.97 mmol) at 0 °C. The mixture was stirred overnight at 25 °C, and then LiOH·H$_2$O (20 mg, 0.48 mmol) was added again to adjust the pH to 9–10. After 3 h, 5% NaHCO$_3$ was added to the reaction mixture. The aqueous layer was washed with Et$_2$O and then acidified to pH 2 using 2 N HCl. The mixture was extracted with Et$_2$O, and the organic layer was dried over Na$_2$SO$_4$. The solvent was removed in vacuo to yield 290 mg (quantitative) of **3c** as a colorless oil which was used directly for the next step without further purification. ^{1}H NMR (300 MHz, CDCl$_3$) δ: 1.21–1.45 (m, 2H), 1.61 (s, 3H), 1.79–1.90 (m, 1H), 2.01–2.12 (m, 3H), 4.94–5.03 (m, 2H), 5.09 (s, 2H), 5.52 (s, 1H), 5.61–5.87 (m, 1H), 7.26–7.36 (m, 5H). ^{13}C NMR (100 MHz, CD$_3$OD): δ 23.9, 24.3, 36.7, 38.0, 60.5, 67.9, 115.8, 129.2, 129.5, 130.0, 138.9, 140.0, 157.9, 178.0. $[\alpha]^{20}_D$ +8.2 (c 1.0, CHCl$_3$). ESI m/z: calcd 291.2 for C$_{16}$H$_{21}$NO$_4$, found 291.0.

Compounds **3a**, **3b**, and **3d** were prepared according to procedures similar to that for **3c**.

(S)-2-(Benzyloxycarbonylamino)-2-methylpent-4-enoic Acid (3a). Starting from **2a** (762 mg, 2.17 mmol), LiOH·H$_2$O (228 mg, 5.42 mmol), and 40 mL of THF/H$_2$O (3/1, v/v), **3a** (579 mg) was obtained as a colorless oil in quantitative yield. ^{1}H NMR (300 MHz, CDCl$_3$) δ: 1.61 (s, 3H), 2.62–2.69 (m, 1H), 2.75–2.77 (m, 1H), 5.06–5.16 (m, 4H), 5.48 (s, 1H), 5.63–5.77 (m, 1H), 7.29–7.39 (m, 5H).

(S)-2-(Benzyloxycarbonylamino)-2-methylbut-4-enoic Acid (3b). Starting from **2b** (366 mg, 1.9 mmol), LiOH·H$_2$O (126 mg, 3 mmol), and 20 mL of THF/H$_2$O (3/1, v/v), **3b** (260 mg) was obtained as a colorless oil in 94% yield.

(S)-2-(Benzyloxycarbonylamino)-2-methyloct-7-enoic Acid (3d). Starting from **2d** (896 mg, 2.28 mmol), LiOH·H$_2$O (239 mg, 5.69 mmol), and 40 mL of THF/H$_2$O (3/1, v/v), **3d** (588 mg) was obtained as a colorless oil in 85% yield. ^{1}H NMR (300 MHz, DMSO-d_6): δ 1.08–1.27 (m, 4H), 1.31 (s, 3H), 1.64–1.76 (m, 2H), 1.98 (q, J = 7.2 Hz, J = 6.6 Hz), 4.90–5.03 (m, 4H), 5.70–5.83 (m, 1H), 7.20–7.44 (m, 5H).

(S)-N-(9-Fluorenylmethyl carbamate)-2-(2′-pentenyl)alanine (4c). To a solution of 2-(benzyloxycarbonylamino)-2-methylhept-6-enoic acid **3c** (169 mg, 0.58 mmol) in 7.5 mL of DME and 4.5 mL of water (DME/H$_2$O = 5:3) was added Ba(OH)$_2$·8H$_2$O (733 mg, 2.32 mmol). After refluxing under nitrogen (65–90 °C) overnight, the mixture was cooled to room temperature, and the barium salts were precipitated. After addition of 8 mL of acetone and 5 mL of H$_2$O and K$_2$CO$_3$ to adjust the pH to 9–10, Fmoc-OSu (216 mg, 0.64 mmol) was added to this solution at room temperature. The mixture was stirred for 2 h and kept at pH 9–10 by adding K$_2$CO$_3$. The mixture was then diluted with water and washed with Et$_2$O. The aqueous layer was acidified with 2 N HCl to pH 2 and extracted with Et$_2$O. The combined organic layers were dried (Na$_2$SO$_4$) and evaporated. The residue was purified by flash column chromatography with elution of CH$_2$Cl$_2$/CH$_3$OH (5:1) to give compound **4c** (130 mg, overall yield of 59% for two steps) as a white solid: $[\alpha]^{20}_D$ +10.6° (c 0.66, CHCl$_3$). ^{1}H NMR (300 MHz, DMSO-d_6) δ 1.33 (m, 5H), 1.99 (t, J = 6.9 Hz, 2H), 4.21–4.27 (m, 3H), 4.94–5.03 (m, 2H), 5.73–5.82 (m, 1H), 7.33 (td, J = 7.2 Hz, 2H), 7.43 (t, J = 7.5 Hz, 2H), 7.72 (d, J = 7.8 Hz, 2H), 7.89 (d, J = 7.6 Hz, 2H). EI-MS m/z: 379 (M$^+$).

Compounds **4a**, **4b**, and **4d** were prepared according to procedures similar to that for **4c**.

(S)-2-(((9H-Fluoren-9-yl)methoxy)carbonylamino)-2-methylpent-4-enoic Acid (4a). Starting from **3a** (238 mg, 0.9 mmol), Ba(OH)$_2$·8H$_2$O (998 mg, 3.2 mmol), 21 mL of DME/H$_2$O (5/3, v/v), and Fmoc-OSu (364 mg, 1.08 mmol), **4a** (231 mg) was obtained as a white powder in 73% yield. ^{1}H NMR (300 MHz, (CD$_3$)$_2$SO) δ: 1.27 (s, 3H), 2.35–2.42 (m, 1H), 2.49–2.60 (m, 1H), 4.19–4.27 (m, 3H), 4.99–5.06 (m, 2H), 5.62–5.71 (m, 1H), 7.28–7.47 (m, 4H), 7.69 (d, 2H, J = 7.5 Hz), 7.86 (d, 2H, J = 7.5 Hz).

(S)-2-(((9H-Fluoren-9-yl)methoxy)carbonylamino)-2-methylbut-5-enoic Acid (4b). Starting from **3b** (260 mg, 0.94 mmol), Ba(OH)$_2$·8H$_2$O (1.035 g, 3.28 mmol), 24 mL of DME/H$_2$O (5/3, v/v), and Fmoc-OSu (364 mg, 1.08 mmol), **4b** (324 mg) was obtained as a white powder in 94% yield. $[\alpha]^{20}_D$ +7.0° (c 1.02, CHCl$_3$). ^{1}H

NMR (300 MHz, DMSO-d_6) δ: 1.33 (s, 3H), 1.72−1.78 (m, 1H), 1.84−1.96 (m, 2H), 4.17−4.27 (m, 3H), 4.92−5.02 (m, 2H), 5.73−5.82 (m, 1H), 7.29−7.34 (m, 2H), 7.39−7.50 (m, 2H), 7.71 (d, 2H, J = 7.8 Hz), 7.88 (d, 2H, J = 7.2 Hz). EI-MS m/z: 365 (M$^+$).

(S)-2-(((9H-Fluoren-9-yl)methoxy)carbonylamino)-2-methyl-oct-7-enoic Acid (4d). Starting from **3d** (274 mg, 0.90 mmol), Ba(OH)$_2$·8H$_2$O (708 mg, 2.24 mmol), 15.1 mL of DME/H$_2$O (5/3, v/v), and Fmoc-OSu (363 mg, 1.08 mmol), **4d** (268 mg) was obtained as a white powder in 76% yield. ^{1}H NMR (300 MHz, DMSO-d_6) δ: 1.11−1.29 (m, 7H), 1.61−1.77 (m, 2H), 1.97 (q, 2H, J = 6.6 Hz), 4.14−4.24 (m, 3H), 4.87−4.99 (m, 2H), 5.67−5.81 (m, 1H), 7.27−7.41 (m, 4H), 7.68 (t, 2H, J = 7.5 Hz), 7.86 (d, 2H, J = 7.8 Hz).

Peptide Synthesis and Characterization. The linear peptides were synthesized manually or instrumentally (CEM Liberty peptide synthesizer) using Fmoc-based SPS protocols on PAL amide resin (0.53 mmol/g) or Rink amide−MBHA resin. The N-Fmoc group of the resin was removed with 20% piperidine in DMF (30 min at room temperature), then coupled with N^α-protected amino acid (3 equiv) in the presence of DIPCDI (3 equiv) and HOBt or HOAt (3 equiv) at room temperature for 2 h. The cycle of deprotection and coupling was repeated until the whole sequence was assembled. The side chain protections of the Fmoc-AA are as follows: Arg(Pmc), Lys(Boc), Thr(t-Bu), Tyr(t-Bu), Trp(Boc). DIPCDI/HOBt (or HOAt) activation of N^α-protected amino acids was employed for the coupling, and 20% piperidine/DMF was used for Fmoc deprotection. TFA/EDT(or TES)/H$_2$O (9.5:0.25:0.25) was used for the resin cleavage and side chain deblocking. For α,α-disubstituted amino acids, double coupling using HOAt was conducted to achieve a complete reaction. The crude peptides were purified to homogeneity by reverse-phase high-performance liquid chromatography (RP-HPLC). HPLC conditions were as follows: Vydac C18 column (10 mm × 250 mm); solvent A, 0.05% TFA in water; solvent B, 0.05% TFA in 95% acetonitrile in water with gradient indicated below; flow rate, 2.5 mL/min; UV detector, 225 nm. ESI-MS was performed on a Finnigan LCQDeca mass spectrometer. The purity of products was characterized by analytical HPLC and ESI-MS and was >98% as determined by HPLC analyses with Vydac 218TP C18 column (4.6 mm × 250 mm) in two solvent systems (system 1, solvent A, 0.05% TFA in water; solvent B, 0.05% TFA in 95% acetonitrile; system 2, solvent A, 0.05% TFA in water; solvent B 0.05% TFA in methanol).

NLH2. t_R = 18.9 min (gradient: 10−20% B over 2 min, 20−60% B over 20 min). ESI-MS m/z (C$_{77}$H$_{116}$N$_{18}$O$_{13}$, calcd 1500.9): 1502.4 ([M + H]$^+$), 752.1 ([M + 2H]$^{2+}$/2). Yield: 65%. Purity: 100% (determined by HPLC).

NLH5. t_R = 22.5 min (gradient: 10−20% B over 2 min, 20−60% B over 20 min). ESI-MS m/z (C$_{78}$H$_{118}$N$_{18}$O$_{14}$, calcd 1530.9): 1532.2 ([M + H]$^+$), 1554.2 ([M + Na]$^+$), 766.8 ([M + 2H]$^{2+}$/2), 1530.1 ([M − H]$^-$). Yield: 61%. Purity: 100% (determined by HPLC).

NLH8. t_R = 26.2 min (gradient: 10−20% B over 2 min, 20−60% B over 20 min). ESI-MS m/z (C$_{75}$H$_{110}$N$_{14}$O$_{14}$ calcd 1430.8): 1431.8 ([M + H]$^+$), 1454.1 ([M + Na]$^+$), 1430.1 ([M − H]$^-$). Yield: 34%. Purity: 100% (determined by HPLC).

NLH10. t_R = 23.4 min (gradient: 0−20% B over 2 min, 20−55% B over 26 min). ESI-MS m/z (C$_{74}$H$_{110}$N$_{18}$O$_{14}$, calcd 1474.8): 1476.2 ([M + H]$^+$), 1474.1 ([M − H]$^-$). Purity: 100% (determined by HPLC).

NLH11. t_R = 16.9 min (gradient: 10−20% B over 2 min, 20−53% B over 18 min). ESI-MS m/z (C$_{76}$H$_{114}$N$_{18}$O$_{14}$, calcd 1503.9): 753.1 ([M + 2H]$^{2+}$/2). Yield: 75%. Purity: 100% (determined by HPLC).

NLH13. t_R = 28.2 min (gradient: 10−22% B over 2 min, 22−60% B over 23 min, 60−90% B over 3 min). ESI-MS m/z (C$_{80}$H$_{122}$N$_{18}$O$_{14}$, calcd 1558.9): 1560.2 ([M + H]$^+$), 1582.2 ([M + Na]$^+$), 781.1 ([M + 2H]$^{2+}$/2). Yield: 42%. Purity: 100% (determined by HPLC).

NLH15. t_R = 28.2 min (gradient: 10−20% B over 2 min, 20−60% B over 23 min). ESI-MS m/z (C$_{78}$H$_{117}$N$_{17}$O$_{14}$, calcd 1515.9): 1517.1 ([M + H]$^+$), 1538.9 ([M + Na]$^+$), 1514.9 ([M − H]$^-$). Yield: 96%. Purity: 100% (determined by HPLC).

Stapled Peptides. By use of the fluorenylmethoxycarbonyl (Fmoc) protection strategy, the linear peptide was synthesized manually on the PAL amide resin coupled with the respective amino acids, and the N-Fmoc group in the N-terminus of the resin-bound peptide was removed with 20% piperidine/DMF (12 min). Then the side chain protected resin-bound peptide was mixed with the Grubbs catalyst (second generation) (0.2 equiv). The reaction mixture was stirred at room temperature for 5 h for peptides **NLH3**, **NLH6**, and **NLH9** or under microwave irradiation (23 W, 75 °C) for 3 min for peptides **NLH14** and **NLH16** in the solvent 1,2-dichloroethane. The peptide was then cleaved from the resin, and meanwhile the side chains were deprotected using the cleavage system: TFA/EDT/H$_2$O (9.5:0.25:0.25) or TFA/TES/H$_2$O (9.5:0.25:0.25) at room temperature for 2 h. The crude peptides were purified to homogeneity by RP-HPLC.

NLH3. t_R = 16.7 min (gradient: 10−20% B over 2 min, 20−60% B over 20 min). ESI-MS m/z (C$_{75}$H$_{112}$N$_{18}$O$_{13}$, calcd 1472.9): 1474.1 ([M + H]$^+$), 737.9 ([M + 2H]$^{2+}$/2), 1472.1 ([M − H]$^-$). Yield: 58%. Purity: 100% (determined by HPLC).

NLH6. t_R = 21.3 min (gradient: 10−20% B over 2 min, 20−60% B over 20 min). ESI-MS m/z (C$_{76}$H$_{114}$N$_{18}$O$_{14}$, calcd 1502.9): 1504.1 ([M + H]$^+$), 752.9 ([M + 2H]$^{2+}$/2), 1502.0 ([M − H]$^-$). Yield: 57%. Purity: 100% (determined by HPLC).

NLH9. t_R = 26.8 min (gradient: 10−20% B over 2 min, 20−60% B over 20 min). ESI-MS m/z (C$_{73}$H$_{106}$N$_{14}$O$_{14}$, calcd 1402.8): 1426.1 ([M + Na]$^+$), 1402.2 ([M − H]$^-$). Yield: 43%. Purity: 100% (determined by HPLC).

NLH12. t_R = 15.19 min (gradient: 10−20% B over 2 min, 20−53% B over 18 min). ESI-MS m/z (C$_{74}$H$_{110}$N$_{18}$O$_{14}$, calcd 1474.9): 1475.9 ([M + H]$^+$), 1473.9 ([M − H]$^-$). Yield: 25%. Purity: 100% (determined by HPLC).

NLH14. t_R = 26.6 min (gradient: 10−22% B over 2 min, 22−60% B over 23 min, 60−90% B over 3 min). ESI-MS m/z (C$_{74}$H$_{110}$N$_{18}$O$_{14}$, calcd 1530.9): 1531.8 ([M + H]$^+$), 1553.8 ([M + Na]$^+$), 777.8 ([M + Na + H]$^{2+}$/2), 766.7 ([M + 2H]$^{2+}$/2). Yield: 43%. Purity: 100% (determined by HPLC).

NLH16. t_R = 16.11 min (gradient: 10−30% B over 2 min, 30−53% B over 23 min). ESI-MS m/z (C$_{76}$H$_{113}$N$_{17}$O$_{14}$, calcd 1487.9): 1489.0 ([M + H]$^+$), 1486.9 ([M − H]$^-$). Yield: 40%. Purity: 100% (determined by HPLC).

Fluorescein-Labeled Peptides. After the N^α-Fmoc deprotection, the side chain protected resin-bound peptide (**NLH-6** or **NL-6**) was coupled with 5-carboxyfluorescein by using DIC and HOBt as the coupling reagents under microwave irradiation (23 W, 75 °C, 10 min) and double coupling. Then treatment of the resin-bound peptide with the cleavage cocktail afforded the fluorescently labeled stapled or linear peptide (**NLX-1** or **NLX-2**).

NLX1. t_R = 19.8 min (gradient: 10−20% B over 2 min, 20−60% B over 20 min). ESI-MS m/z (C$_{97}$H$_{124}$N$_{18}$O$_{20}$, calcd 1862.1): 1862.9 ([M + H]$^+$), Yield: 72%. Purity: 100% (determined by HPLC).

NLX2. t_R = 16.8 min (gradient: 10−20% B over 2 min, 20−60% B over 20 min). ESI-MS m/z (C$_{92}$H$_{118}$N$_{18}$O$_{20}$, calcd 1796.1): 1796.9 ([M + H]$^+$). Yield: 37%. Purity: 99% (determined by HPLC).

■ ASSOCIATED CONTENT

Ⓢ Supporting Information

Details of circular dichroism (CD) measurements, in vitro assay for HIV-1 IN catalytic activity inhibition, in vitro assay for inhibition of LEDGF/p75-HIV-1 IN interaction, and confocal microscopy protocol and ^{1}H NMR spectra of the alkylation products **2**. This material is available free of charge via the Internet at http://pubs.acs.org.

■ AUTHOR INFORMATION

Corresponding Author

*For Y.-Q.L.: phone, 86-21-50806876; fax, +86-21-50806876; e-mail, yqlong@mail.shcnc.ac.cn. For N.N.: phone, 323-442-2341; fax, 323-442-1390; e-mail, neamati@usc.edu.

Author Contributions

$^\|$S.-X.H. and Z.Z. contributed equally to this manuscript.

■ ABBREVIATIONS USED

Cbz, carboxybenzoyl; CD, circular dichroism; CC_{50}, cytotoxic concentration 50%; DIPCDI, diisopropylcarbodiimide; DME, dimethyl ether; EC_{50}, effective concentration 50%; EDT, 1,2-ethanedithiol; Fmoc, fluorenylmethoxycarbonyl; HIV-1 IN, human immunodeficiency virus type 1 integrase; IBD, integrase binding domain; LEDGF, lens epithelium-derived growth factor; LDA, lithium diisopropylamide; LDEA, lithium diethylamide; LiHMDS, lithium bis(trimethylsilyl)amide; KHMDS, lithium hexamethyldisilazide; PBS, phosphate buffered saline; PIC, preintegration complex; RCM, ring-closing metathesis; THF/HMPA, tetrahydrofuran/hexamethylphosphoramide; THF/DME, tetrahydrofuran/ethylene glycol dimethyl ether; TES, triethylsilane; TFA, trifluoroacetic acid; TFE, trifluoroethanol; TI, therapeutic index; TMS, tetramethylsilane

■ REFERENCES

(1) Asante-Appiah, E.; Skalka, A. M. HIV-1 integrase: structural organization, conformational changes, and catalysis. *Adv. Virus Res.* **1999**, *52*, 351−369.

(2) Brown, P. O. *Integration in Retroviruses*; Coffin, J. M., Hughes, S. H., Varmus, H. E., Eds.; Cold Spring Harbor Laboratory Press: Cold Spring Harbor, NY, 1997; pp 161−203.

(3) Craigie, R. Integrase Mechanism and Function. In *HIV-1 Integrase: Mechanism and Inhibitor Design*; Neamati, N., Ed.; Wiley: Hoboken, NJ, 2011.

(4) Permpalung, N.; Putcharoen, O.; Avihingsanon, A.; Ruxrungtham, K. Treatment of HIV infection with once-daily regimens. *Expert Opin. Pharmacother.* **2012**, *13*, 2301−2317.

(5) van Lunzen, J.; Maggiolo, F.; Arribas, J. R.; Rakhmanova, A.; Yeni, P.; Young, B.; Rockstroh, J. K.; Almond, S.; Song, I.; Brothers, C.; Min, S. Once daily dolutegravir (S/GSK1349572) in combination therapy in antiretroviral-naive adults with HIV: planned interim 48 week results from SPRING-1, a dose-ranging, randomised, phase 2b trial. *Lancet Infect. Dis.* **2012**, *12*, 111−118.

(6) Underwood, M. R.; Johns, B. A.; Sato, A.; Martin, J. N.; Deeks, S. G.; Fujiwara, T. The activity of the integrase inhibitor dolutegravir against HIV-1 variants isolated from raltegravir-treated adults. *JAIDS, J. Acquired Immune Defic. Syndr.* **2012**, *61*, 297−301.

(7) Dooley, K. E.; Sayre, P.; Borland, J.; Purdy, E.; Chen, S. G.; Song, I.; Peppercorn, A.; Everts, S.; Piscitelli, S.; Flexner, C. Safety, tolerability, and pharmacokinetics of the HIV Integrase inhibitor dolutegravir given twice daily with rifampin or once daily with rifabutin: results of a phase 1 study among healthy subjects. *JAIDS, J. Acquired Immune Defic. Syndr.* **2013**, *62*, 21−27.

(8) Thys, W.; Bartholomeeusen, K.; Debyser, Z.; De Rijck, J. Cellular Cofactors of HIV Integration. In *HIV-1 Integrase: Mechanism and Inhibitor Design*; Neamati, N., Ed.; Wiley: Hoboken, NJ, 2011.

(9) Cherepanov, P.; Maertens, G.; Proost, P.; Devreese, B.; Van Beeumen, J.; Engelborghs, Y.; De Clercq, E.; Debyser, Z. HIV-1 integrase forms stable tetramers and associates with LEDGF/p75 protein in human cells. *J. Biol. Chem.* **2003**, *278*, 372−381.

(10) Engelman, A.; Cherepanov, P. The lentiviral integrase binding protein LEDGF/p75 and HIV-1 replication. *PLoS Pathog.* **2008**, *4*, e1000046.

(11) Hamamoto, S.; Nishitsuji, H.; Amagasa, T.; Kannagi, M.; Masuda, T. Identification of a novel human immunodeficiency virus type 1 integrase interactor, Gemin2, that facilitates efficient viral cDNA synthesis in vivo. *J. Virol.* **2006**, *80*, 5670−5677.

(12) Al-Mawsawi, L. Q.; Neamati, N. Blocking HIV-1 integrase-cellular cofactor interactions: an emerging anti-retroviral strategy. *Trends Pharmacol. Sci.* **2007**, *28*, 526−535.

(13) Krishnan, L.; Matreyek, K. A.; Oztop, I.; Lee, K.; Tipper, C. H.; Li, X.; Dar, M. J.; Kewalramani, V. N.; Engelman, A. The requirement for cellular transportin 3 (TNPO3 or TRN-SR2) during infection maps to human immunodeficiency virus type 1 capsid and not integrase. *J. Virol.* **2010**, *84*, 397−406.

(14) Christ, F.; Thys, W.; De Rijck, J.; Gijsbers, R.; Albanese, A.; Arosio, D.; Emiliani, S.; Rain, J. C.; Benarous, R.; Cereseto, A.; Debyser, Z. Transportin-SR2 imports HIV into the nucleus. *Curr. Biol.* **2008**, *18*, 1192−1202.

(15) Zhang, J.; Scadden, D. T.; Crumpacker, C. S. Primitive hematopoietic cells resist HIV-1 infection via p21. *J. Clin. Invest.* **2007**, *117*, 473−481.

(16) Zawahir, Z.; Neamati, N. Inhibition of HIV-1 integrase activity by synthetic peptides derived from the HIV-1 HXB2 Pol region of the viral genome. *Bioorg. Med. Chem. Lett.* **2006**, *16*, 5199−5202.

(17) Li, H. Y.; Zawahir, Z.; Song, L. D.; Long, Y. Q.; Neamati, N. Sequence-based design and discovery of peptide inhibitors of HIV-1 integrase: insight into the binding mode of the enzyme. *J. Med. Chem.* **2006**, *49*, 4477−4486.

(18) Al-Mawsawi, L. Q.; Christ, F.; Dayam, R.; Debyser, Z.; Neamati, N. Inhibitory profile of a LEDGF/p75 peptide against HIV-1 integrase: insight into integrase-DNA complex formation and catalysis. *FEBS Lett.* **2008**, *582*, 1425−1430.

(19) Al-Mawsawi, L. Q.; Fikkert, V.; Dayam, R.; Witvrouw, M.; Burke, T. R., Jr.; Borchers, C. H.; Neamati, N. Discovery of a small-molecule HIV-1 integrase inhibitor-binding site. *Proc. Natl. Acad. Sci. U.S.A.* **2006**, *103*, 10080−10085.

(20) Wang, J. Y.; Ling, H.; Yang, W.; Craigie, R. Structure of a two-domain fragment of HIV-1 integrase: implications for domain organization in the intact protein. *EMBO J.* **2001**, *20*, 7333−7343.

(21) Dyda, F.; Hickman, A. B.; Jenkins, T. M.; Engelman, A.; Craigie, R.; Davies, D. R. Crystal-structure of the catalytic domain of HIV-1 integrase: similarity to other polynucleotidyl transferases. *Science* **1994**, *266*, 1981−1986.

(22) Chen, H.; Engelman, A. Characterization of a replication-defective human immunodeficiency virus type 1 att site mutant that is blocked after the 3′ processing step of retroviral integration. *J. Virol.* **2000**, *74*, 8188−8193.

(23) Hwang, D. J.; Kim, S. N.; Choi, J. H.; Lee, Y. S. Dicaffeoyl- or digalloyl pyrrolidine and furan derivatives as HIV integrase inhibitors. *Bioorg. Med. Chem.* **2001**, *9*, 1429−1437.

(24) Schafmeister, C. E.; Po, J.; Verdine, G. L. An all-hydrocarbon cross-linking system for enhancing the helicity and metabolic stability of peptides. *J. Am. Chem. Soc.* **2000**, *122*, 5891−5892.

(25) Walensky, L. D.; Kung, A. L.; Escher, I.; Malia, T. J.; Barbuto, S.; Wright, R. D.; Wagner, G.; Verdine, G. L.; Korsmeyer, S. J. Activation of apoptosis in vivo by a hydrocarbon-stapled BH3 helix. *Science* **2004**, *305*, 1466−1470.

(26) Walensky, L. D.; Pitter, K.; Morash, J.; Oh, K. J.; Barbuto, S.; Fisher, J.; Smith, E.; Verdine, G. L.; Korsmeyer, S. J. A stapled BID BH3 helix directly binds and activates BAX. *Mol. Cell* **2006**, *24*, 199−210.

(27) Okamoto, T.; Zobel, K.; Fedorova, A.; Quan, C.; Yang, H.; Fairbrother, W. J.; Huang, D. C.; Smith, B. J.; Deshayes, K.; Czabotar, P. E. Stabilizing the pro-apoptotic BimBH3 helix (BimSAHB) does not necessarily enhance affinity or biological activity. *ACS Chem. Biol.* **2013**, *8*, 297−302.

(28) Bernal, F.; Tyler, A. F.; Korsmeyer, S. J.; Walensky, L. D.; Verdine, G. L. Reactivation of the p53 tumor suppressor pathway by a stapled p53 peptide. *J. Am. Chem. Soc.* **2007**, *129*, 2456−2457.

(29) Baek, S.; Kutchukian, P. S.; Verdine, G. L.; Huber, R.; Holak, T. A.; Lee, K. W.; Popowicz, G. M. Structure of the stapled p53 peptide bound to Mdm2. *J. Am. Chem. Soc.* **2012**, *134*, 103−106.

(30) Zhang, H.; Zhao, Q.; Bhattacharya, S.; Waheed, A. A.; Tong, X.; Hong, A.; Heck, S.; Curreli, F.; Goger, M.; Cowburn, D.; Freed, E. O.; Debnath, A. K. A cell-penetrating helical peptide as a potential HIV-1 inhibitor. *J. Mol. Biol.* **2008**, *378*, 565−580.

(31) Foged, C.; Franzyk, H.; Bahrami, S.; Frokjaer, S.; Jaroszewski, J. W.; Nielsen, H. M.; Olsen, C. A. Cellular uptake and membrane-destabilising properties of alpha-peptide/beta-peptoid chimeras: lessons for the design of new cell-penetrating peptides. *Biochim. Biophys. Acta* **2008**, *1778*, 2487−2495.

(32) Fawell, S.; Seery, J.; Daikh, Y.; Moore, C.; Chen, L. L.; Pepinsky, B.; Barsoum, J. Tat-mediated delivery of heterologous proteins into cells. *Proc. Natl. Acad. Sci. U.S.A.* **1994**, *91*, 664−668.

(33) Hayouka, Z.; Hurevich, M.; Levin, A.; Benyamini, H.; Iosub, A.; Maes, M.; Shalev, D. E.; Loyter, A.; Gilon, C.; Friedler, A. Cyclic peptide inhibitors of HIV-1 integrase derived from the LEDGF/p75 protein. *Bioorg. Med. Chem.* **2010**, *18*, 8388−8395.

(34) Desimmie, B. A.; Humbert, M.; Lescrinier, E.; Hendrix, J.; Vets, S.; Gijsbers, R.; Ruprecht, R. M.; Dietrich, U.; Debyser, Z.; Christ, F. Phage display-directed discovery of LEDGF/p75 binding cyclic peptide inhibitors of HIV replication. *Mol. Ther.* **2012**, *20*, 2064−2075.

(35) Hayouka, Z.; Levin, A.; Hurevich, M.; Shalev, D. E.; Loyter, A.; Gilon, C.; Friedler, A. A comparative study of backbone versus side chain peptide cyclization: application for HIV-1 integrase inhibitors. *Bioorg. Med. Chem.* **2012**, *20*, 3317−3322.

(36) Li, P.; Roller, P. P. Cyclization strategies in peptide derived drug design. *Curr. Top. Med. Chem.* **2002**, *2*, 325−341.

(37) Li, P.; Roller, P. P.; Xu, J. C. Current synthetic approaches to peptide and peptidomimetic cyclization. *Curr. Org. Chem.* **2002**, *6*, 411−440.

(38) de Vega, M. J. P.; Garcia-Aranda, M. I.; Gonzalez-Muniz, R. A Role for ring-closing metathesis in medicinal chemistry: mimicking secondary architectures in bioactive peptides. *Med. Res. Rev.* **2011**, *31*, 677−715.

(39) Seebach, D.; Fadel, A. *N,O*-Acetals from pivalaldehyde and amino acids for the α-alkylation with self-reproduction of the center of chirality. Enolates of 3-benzoyl-2-(*tert*-butyl)-1,3-oxazolidin-5-ones. *Helv. Chim. Acta* **1985**, *68*, 1243−1250.

(40) Karady, S.; Amato, J. S.; Weinstock, L. M. Enantioretentive alkylation of acyclic amino acids. *Tetrahedron Lett.* **1984**, *25*, 4337−4340.

(41) Altman, E.; Nebel, K.; Mutter, M. Versatile stereoselective synthesis of completely protected trifunctional α-methylated α-amino acids starting from alanine. *Helv. Chim. Acta* **1991**, *74*, 800−806.

(42) Long, Y. Q.; Xue, T.; Song, Y. L.; Liu, Z. L.; Huang, S. X.; Yu, Q. Synthesis and utilization of chiral alpha-methylated alpha-amino acids with a carboxyalkyl side chain in the design of novel Grb2-SH2 peptide inhibitors free of phosphotyrosine. *J. Med. Chem.* **2008**, *51*, 6371−6380.

(43) Kapadia, S. R.; Spero, D. M.; Eriksson, M. An improved synthesis of chiral alpha-(4-bromobenzyl)alanine ethyl ester and its application to the synthesis of LFA-1 antagonist BIRT-377. *J. Org. Chem.* **2001**, *66*, 1903−1905.

(44) Zhang, H.; Kaneko, K.; Nguyen, J. T.; Livshits, T. L.; Baldwin, M. A.; Cohen, F. E.; James, T. L.; Prusiner, S. B. Conformational transitions in peptides containing two putative alpha-helices of the prion protein. *J. Mol. Biol.* **1995**, *250*, 514−526.

(45) Forood, B.; Feliciano, E. J.; Nambiar, K. P. Stabilization of alpha-helical structures in short peptides via end capping. *Proc. Natl. Acad. Sci. U.S.A.* **1993**, *90*, 838−842.

(46) Faure, A.; Calmels, C.; Desjobert, C.; Castroviejo, M.; Caumont-Sarcos, A.; Tarrago-Litvak, L.; Litvak, S.; Parissi, V. HIV-1 integrase crosslinked oligomers are active in vitro. *Nucleic Acids Res.* **2005**, *33*, 977−986.

(47) Guiot, E.; Carayon, K.; Delelis, O.; Simon, F.; Tauc, P.; Zubin, E.; Gottikh, M.; Mouscadet, J. F.; Brochon, J. C.; Deprez, E. Relationship between the oligomeric status of HIV-1 integrase on DNA and enzymatic activity. *J. Biol. Chem.* **2006**, *281*, 22707−22719.

(48) Cherepanov, P.; Ambrosio, A. L. B.; Rahman, S.; Ellenberger, T.; Engelman, A. Structural basis for the recognition between HIV-1 integrase and transcriptional coactivator p75. *Proc. Natl. Acad. Sci. U.S.A.* **2005**, *102*, 17308−17313.

(49) de Vreese, K.; Kofler-Mongold, V.; Leutgeb, C.; Weber, V.; Vermeire, K.; Schacht, S.; Anne, J.; de Clercq, E.; Datema, R.; Werner, G. The molecular target of bicyclams, potent inhibitors of human immunodeficiency virus replication. *J. Virol.* **1996**, *70*, 689−696.

(50) De Clercq, E. The bicyclam AMD3 100 story. *Nat. Rev. Drug Discovery* **2003**, *2*, 581−587.

(51) Henchey, L. K.; Jochim, A. L.; Arora, P. S. Contemporary strategies for the stabilization of peptides in the alpha-helical conformation. *Curr. Opin. Chem. Biol.* **2008**, *12*, 692−697.

(52) Kritzer, J. A. Stapled peptides: magic bullets in nature's arsenal. *Nat. Chem. Biol.* **2010**, *6*, 566−567.

(53) Whelan, J. Stapled peptide induces cancer cell death. *Drug Discovery Today* **2004**, *9*, 907.

(54) Verdine, G. L.; Hilinski, G. J. Stapled peptides for intracellular drug targets. *Methods Enzymol.* **2012**, *503*, 3−33.

(55) Verdine, G. L.; Walensky, L. D. The challenge of drugging undruggable targets in cancer: lessons learned from targeting BCL-2 family members. *Clin. Cancer Res.* **2007**, *13*, 7264−7270.

(56) Pommier, Y.; Johnson, A. A.; Marchand, C. Integrase inhibitors to treat HIV/AIDS. *Nat. Rev. Drug Discovery* **2005**, *4*, 236−248.

(57) Brass, A. L.; Dykxhoorn, D. M.; Benita, Y.; Yan, N.; Engelman, A.; Xavier, R. J.; Lieberman, J.; Elledge, S. J. Identification of host proteins required for HIV infection through a functional genomic screen. *Science* **2008**, *319*, 921−926.